

Research Article

An Optimal Algorithm for Planning Shearer Trailing Drum Cutting Path

Hong Zhang,¹ Yunbing Hou ,¹ Zhenming Sun ,¹ Zhen Li,² Shanjun Mao,³ Mei Li,³ and Jinzheng Wang⁴

¹School of Energy and Mining Engineering, China University of Mining and Technology (Beijing), Beijing 100083, China

²Beijing Longruan Technology Co. Ltd., Beijing 100190, China

³Research Institute of Remote Sensing and Geographical Information System, Peking University, Beijing 100871, China

⁴Guotun Coal Mine, Linyi Mining Group Heze Coal and Electricity Co. Ltd., Heze 274000, China

Correspondence should be addressed to Yunbing Hou; 18801302683@163.com

Received 30 April 2021; Revised 9 July 2021; Accepted 6 August 2021; Published 21 August 2021

Academic Editor: Gong-Da Wang

Copyright © 2021 Hong Zhang et al. This is an open access article distributed under the Creative Commons Attribution License, which permits unrestricted use, distribution, and reproduction in any medium, provided the original work is properly cited.

The intelligent adaptive cutting of the shearer is one of the key technologies to realize the intelligent working face. However, since the “memory cut” technology is the mainstream technology, which cannot actively adapt to the coal seam variations, the trailing drum usually cuts at a fixed height without a planned cutting path. This paper analyzes the shearer’s location characteristics before and after the advancement to propose a complete calculation method for the advancing path of the shearer, which simulates all of its possible advancing paths for subsequent n cuttings. The multitree and depth-first search algorithms are utilized to filter out the optimal advance path under different mining requirements. Simultaneously, this paper indicates that the vertical curvature of the armored face conveyor (AFC) should be considered in the calculation process of the optimal advancing path at different positions of the working face to obtain the shearer’s planned cutting path for subsequent n cuttings. The proposed algorithm in this paper has apparent advantages over the “memory cut” technology and provides a good solution for the intelligent planning of cutting and pitch steering of the shearers.

1. Introduction

Coal is still an important energy source in the world. However, compared with other energy industries, the technological level of the coal industry is relatively backward. The integration is low, the information level is insufficient, the mining environment is dangerous [1, 2], and safety accidents occur from time to time. Therefore, the coal industry’s development trend requires upgrading and optimizing traditional mining technologies and constructing intelligent and unmanned mines based on some technologies, such as the Internet of Things, virtual simulation [3, 4], and big data.

After about 30 years of rapid development, China’s coal industry has made considerable progress in fully mechanized mining equipment manufacturing and mining technologies. Based on the development level of the complete set

of equipment control systems for fully mechanized mining face in terms of perception, decision making, and execution, Wang et al. [5–9] divided the face control system into three stages: automation, intelligence, and unmanned. At present, the face control system is making every effort to move from automation to intelligence with equipment manufacturing and Internet of Things technology.

In order to realize the intelligent adaptive cutting of the shearer, as one of the key technologies to realize the intelligent working face, the high-precision three-dimensional (3D) geological model is necessary. Although the current detection technology is still unable to grasp the coal geological information of the panel entirely, the dynamic coal geological information mastered during the mine construction operation can be utilized to accurately predict the undulation and structure of the coal seam ahead of the working face. Mao [10, 11] proposed the concept of “gray

geographic information system,” which means that as the mining work progresses, coal seam information is gradually mastered, while the 3D coal seam geological model presents a process of “from black to gray, from gray to white.” Cheng [12] proposed the gradient modeling idea. He established four 3D geological models with different accuracy levels according to the coal seam information mastered at different mining stages. They were named the black-box model, gray-box model, white-box model, and transparent model, respectively. Liu [13] proposed a modeling method and a dynamic correction method of “gradient modeling, dynamic correction, step by step iteration, and refinement” based on the above ideas. With the continuous development of modeling methods and the continuous disclosure of geological information, the accuracy of geological models is constantly improving. Although the error still exists, the 3D geological model of the local area ahead of the working face can already be employed to guide production by adding the newly exposed coal seam data at the working face and updating the geological model continuously.

The “memory cut” technology was introduced to America in 1986, in which the data on drum elevation and ranging arm inclination and shearer location were recorded in the training run. Those data were recalled to run the subsequent shearer’s cuts [14, 15]. However, this method can only be mined with fixed mining height. After that, a gamma ray was introduced to measure the coal thickness to adjust the mining height, but it was not realized. At present, the face alignment and the remote control of the working face based on the inertial navigation system (INS) are the primary development directions of the coal shearer’s intelligent control in the United States, Australia, and other countries [16–18]. The development of shearer cutting curve planning is slow. After introducing the “memory cut” technology into China, Tan [19] modified the critical point data to optimize the coal cutting path. Zhang et al. [20–23] employed the genetic algorithm and particle swarm algorithm to analyze the coal cutting path and shearer data to optimize the next cutting path. Then, Wang et al. [24, 25] introduced the artificial immune theory to explain the adaptive adjustment strategy of the coal seam variation area in the memory cutting path. Although these methods optimized the “memory cut” technology, they still could not actively adapt to the coal seam variations, and the cutting path was still optimized on the vertical profile. Thus, Zhou [26] adopted the gray system theory and historical mining height data to establish a gray prediction model for predicting the next cutting height and cutting path. Although the prediction accuracy was inaccurate and the cutting path still should be manually corrected, he has brought the optimization method of cutting path from the 2D vertical profile perspective to the 3D perspective. In the 3D perspective, Si [27] employed the least squares support vector machine (LS-SVM) to predict the thickness of the coal seam and utilized the B-spline curve to fit and optimize the predicted coal seam data to obtain the next cutting path of the shearer. Ge [28] employed geological bodies, precise positioning, and attitude perception technology to propose the shearer autonomous navigation cutting technology to plan the shearer’s

cutting path and adjust the mining height and the face alignment.

Although the optimized “memory cut” technology can accurately predict the cutting path of the next cut, all optimization methods are optimized for the leading drum cutting curve, while the trailing drum still cuts at a fixed height. Moreover, these methods cannot adapt well to the spatial shape variations of the coal seam ahead of the working face. The main reason is that these methods only optimize or predict the next cutting path, and they do not consider the logical constraints between the subsequent successive n cutting paths and the influence of the undulations of the coal seam ahead of the working face on the advance path planning of the shearer in the optimization process. Moreover, these methods do not have a unified plan for the shearer pitch steering and advancing path.

This paper proposes an optimal algorithm for planning the shearer trailing drum cutting path to overcome the existing problems. In order to achieve the maximum recovery, the proposed method employs the local high-precision 3D dynamic geological model to obtain the accurate coal seam bottom boundary data ahead of the working face and comprehensively considers the shearer drum adjustment, the vertical curvature of the armored face conveyor (AFC), the pitch angle of shearer, and the mining technology requirements to plan the cutting path of the shearer trailing drum for subsequent n cuttings.

2. Cutting Path Planning Method

In a full-thickness working face at one time, the shearer should mine along the top and bottom boundaries of the coal seam to mine as much coal as possible and cut as little rock as possible. Given the lack of the control strategy and cutting path of the trailing drum in the “memory cut” technology, this paper proposes an optimal algorithm for planning the cutting path of the shearer trailing drum. Combined with the high-precision 3D dynamic geological model, it can plan the cutting path of the shearer and realize the intelligent control and optimal cutting of the shearer. The main process is shown in Figure 1.

During the mining process, the adjustment of the shearer drum should fully consider the undulations of the coal seam in the two directions of moving and advancing and the limitations of related equipment and mining technology. Thus, it is difficult to calculate the cutting path for subsequent n cuttings directly. Therefore, this paper first considers the path calculation method of the shearer in the advancing direction. Different adjustment values of the shearer trailing drum correspond to different advancing paths. The depth-first search algorithm is utilized to traverse all possible advancing paths, while the areas between the advancing path and coal seam bottom boundary (extracted from the local high-precision 3D dynamic geological model ahead of the working face) are compared to obtain the optimal advancing path. The constraint condition of shearer moving direction is then introduced to calculate the optimal advancing path at different working face positions, and the nodes with the same cutter number in all the optimal advancing paths are

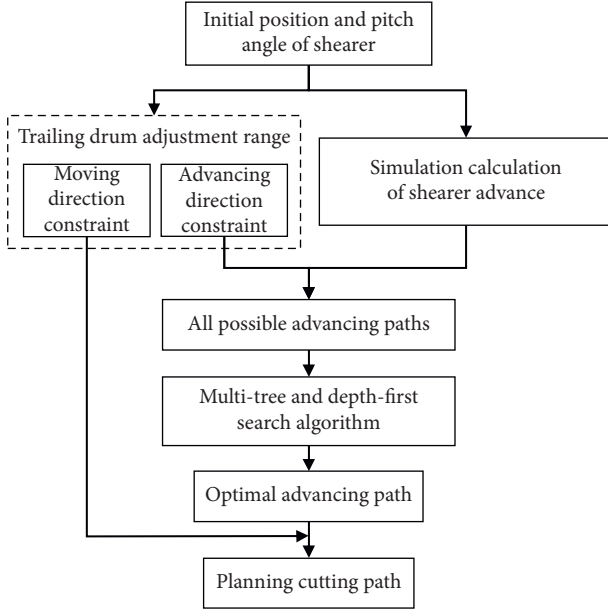


FIGURE 1: Flowchart of the calculation method for planning the cutting path of the trailing drum.

orderly connected to obtain the final cutting path for subsequent n cuttings.

In practical applications, with the advancement of the working face and the continuous dynamic update of the 3D geological model, the cutting path must also be updated simultaneously. On the one hand, it improves the accuracy of the planned cutting path. On the other hand, it ensures that each cutting path is planned considering the coal seam ahead of the work face such that the planned cutting path can better adapt to the coal seam fluctuations.

3. The Adjustment Range of the Shearer Trailing Drum

The adjustment range of the shearer trailing drum is mainly determined by the constraints of the shearer's advancing direction and moving direction.

3.1. Advancing Direction Constraints. The constraints on the advancing direction of the shearer trailing drum are mainly divided into two categories, namely, mechanical equipment and coal mining technology constraints. The mechanical equipment constraints are the pitch angle of the shearer (see Figure 2(a)) and the floor-based quantity (see Figure 2(b)), while the coal mining technology constraint is the height of the floor steps in the advancing direction (see Figure 2(a)).

The floor step is shown in Figure 2. The floor steps of each cutting are connected to form the shearer's advancing path. The slope of the floor step is determined by the pitch angle of the shearer's body during coal cutting, while its position can be adjusted by raising and lowering the trailing drum. However, the following constraints should be considered:

$$\begin{cases} \Delta w < \Delta w_{\max}, \\ \Delta h < \Delta h_{\max}, \end{cases} \quad (1)$$

where Δw and Δh are the floor-based quantity of the shearer and the height of the floor steps, where their maximum values are denoted as Δw_{\max} and Δh_{\max} , respectively. These maximum values are compatible with the performance of the shearer and the technological requirements of the working face, respectively.

Simultaneously, the shearer should meet the following requirements after it is advanced.

$$\alpha < \alpha_{\max}, \quad (2)$$

where α is the pitch angle of the shearer and α_{\max} is the maximum pitch angle.

3.2. Moving Direction Constraints. As shown in Figure 3, the moving direction constraint is the vertical curvature of AFC, where β is the vertical curvature angle.

The vertical curvature of AFC should be considered in the calculation of the adjustment range of the shearer trailing drum. When calculating the advancing path of different positions of the working face, it is necessary to calculate from one face end to the other gradually along the moving direction to ensure that the two adjacent sections of AFC meet the requirements.

$$\beta < \beta_{\max}, \quad (3)$$

where β_{\max} is the maximum vertical curvature angle of AFC, which is compatible with the performance of AFC.

4. Calculation of the Shearer Advancing Path

Although the advancing path of the shearer can be adjusted by raising and lowering the trailing drum, the position and pitch angle of the shearer during coal cutting affect each advancing path significantly. Thus, the position of the shearer determines the position of the advancing path, while the pitch angle determines the slope of the advancing path.

Since the shearer moves on AFC and AFC is placed on the working face bottom plate steadily, the shearer's position and pitch angle are equal to those of the middle groove which is exactly beneath the shearer. The position and pitch angle of the middle groove can be calculated by calculating the front and rear endpoints of the middle groove bottom. Besides, taking the upward inclined mining as an example, there are four contact states between AFC and the floor plate due to floor steps, as shown in Figure 4.

A different method should be employed to calculate the position and pitch angle of AFC for a different contact state between AFC and the working face bottom plate. Since the advancement process of AFC is an orderly continuous process, the position of AFC after the advancement can be calculated according to the position data before the advancement.

Figure 5 shows a schematic diagram of the advancing process of AFC from the position of the i^{th} cutting to the

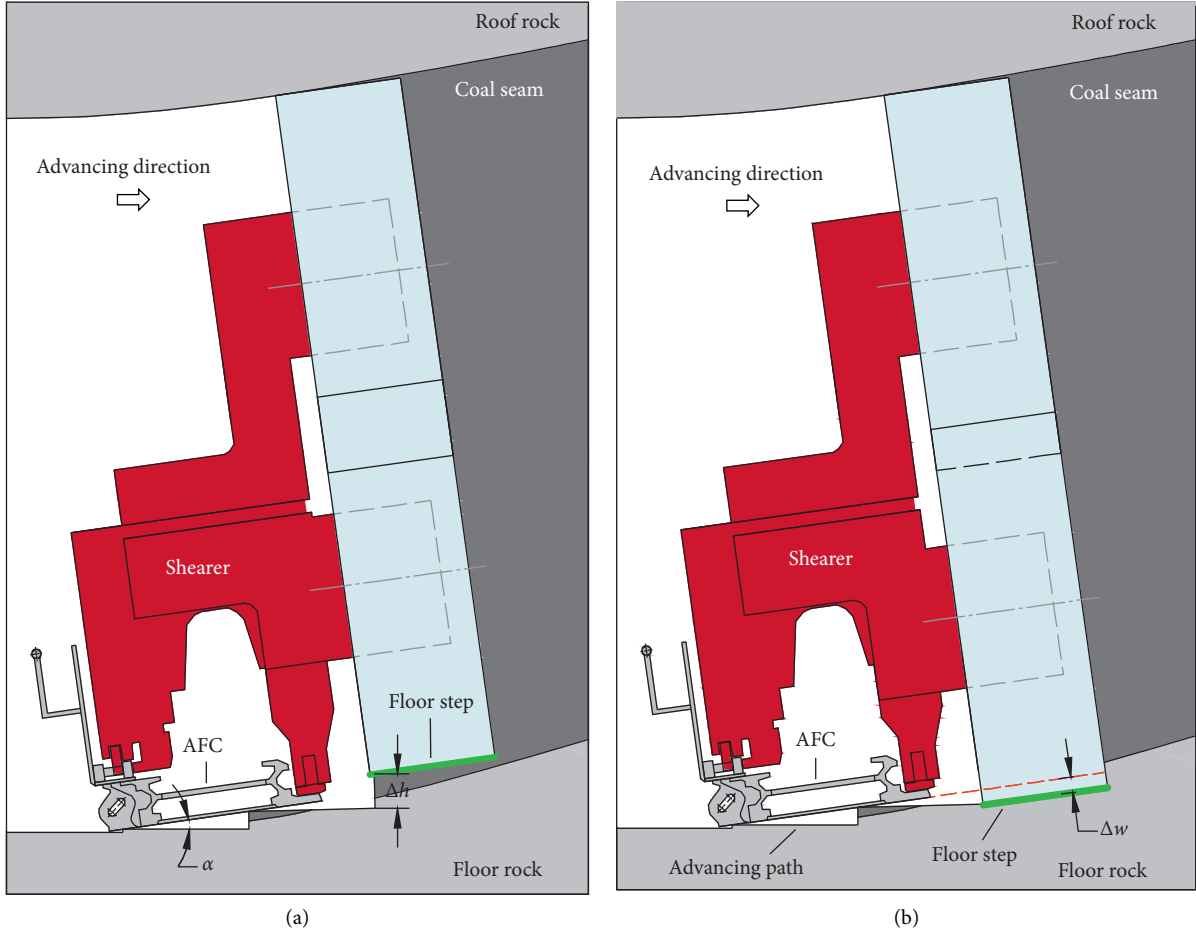


FIGURE 2: Schematic diagram of the constraints in advancing direction.

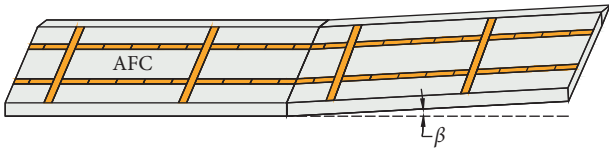


FIGURE 3: Schematic diagram of the vertical curvature of AFC.

position of the $i + 1^{\text{th}}$ cutting. For easy understanding, it is assumed that the advancing direction of AFC is the x -axis, while the vertical direction is the z -axis. S is the cutting depth of the shearer or the one-time advance distance of AFC. L is the width of AFC. B_i and A_i are the front and rear endpoints of the AFC bottom during the i^{th} cutting, respectively. D_i and C_i describe the front and rear endpoints of the i^{th} advancing path. E_i indicates the high point between points C_i and D_{i-1} . k_i is the slope of the i^{th} floor step or the pitch slope of AFC during the i^{th} cutting.

AFC advances by one step. If the effect of the floor step is not considered, AFC will be pushed from the position $A_i B_i$ to $A_{i+1}' B_{i+1}'$. The following equations can calculate the coordinates of point A_{i+1}' and point B_{i+1}' :

$$\begin{cases} (x_{A_{i+1}'} - x_{A_i})^2 + (z_{A_{i+1}'} - z_{A_i})^2 = S^2, \\ \frac{z_{A_{i+1}'} - z_{C_{i-2}}}{x_{A_{i+1}'} - x_{C_{i-2}}} = k_{i-2}, \\ x_{A_{i+1}'} > x_{C_{i-2}}, \end{cases} \quad (4)$$

$$\begin{cases} (x_{B_{i+1}'} - x_{A_{i+1}'})^2 + (z_{B_{i+1}'} - z_{A_{i+1}'})^2 = L^2, \\ \frac{z_{B_{i+1}'} - z_{C_i}}{x_{B_{i+1}'} - x_{C_i}} = k_i, \\ x_{B_{i+1}'} > x_{C_i}. \end{cases}$$

If the effect of the floor step is considered, the straight line between point A_{i+1}' and point B_{i+1}' is chosen as $f(x)$, while $F(X) = z_X - f(x_X)$. $F(E_{i-1})$ and $F(E_i)$ are obtained as

$$\begin{cases} F(E_{i-1}) = z_{E_{i-1}} - f(x_{E_{i-1}}), \\ F(E_i) = z_{E_i} - f(x_{E_i}). \end{cases} \quad (5)$$

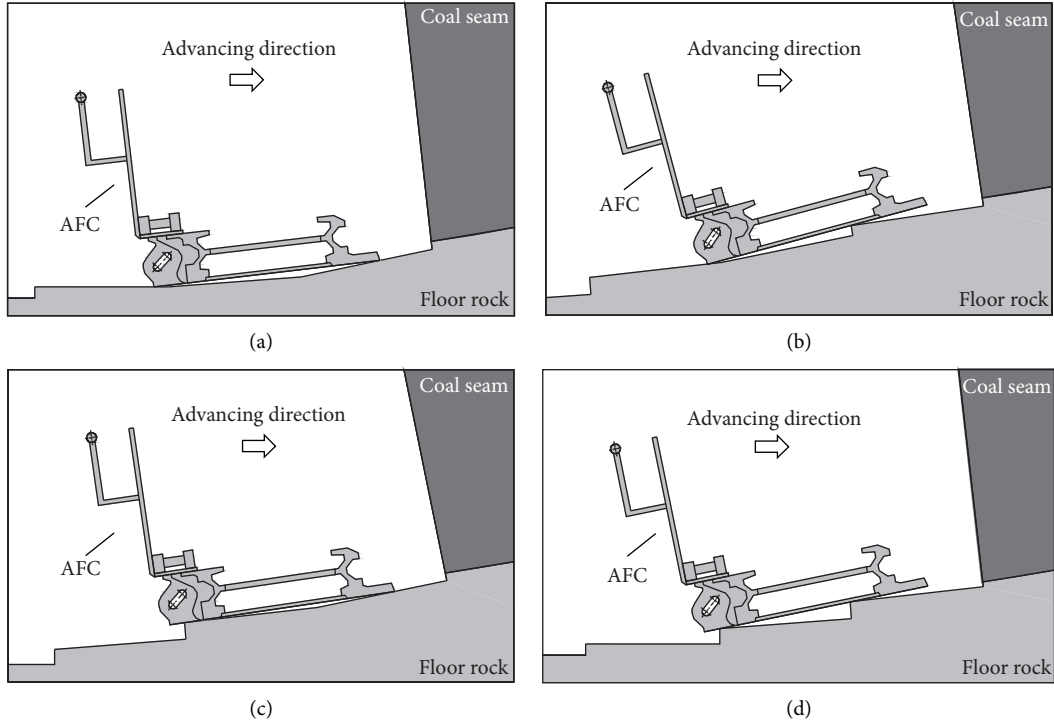


FIGURE 4: Schematic diagram of different contact states between AFC and the floor plate: (a) two endpoints of the AFC bottom contact the floor plate; (b) the rear endpoint contacts the floor plate; (c) the front endpoint contacts the floor plate; (d) no endpoint contacts the floor plate.

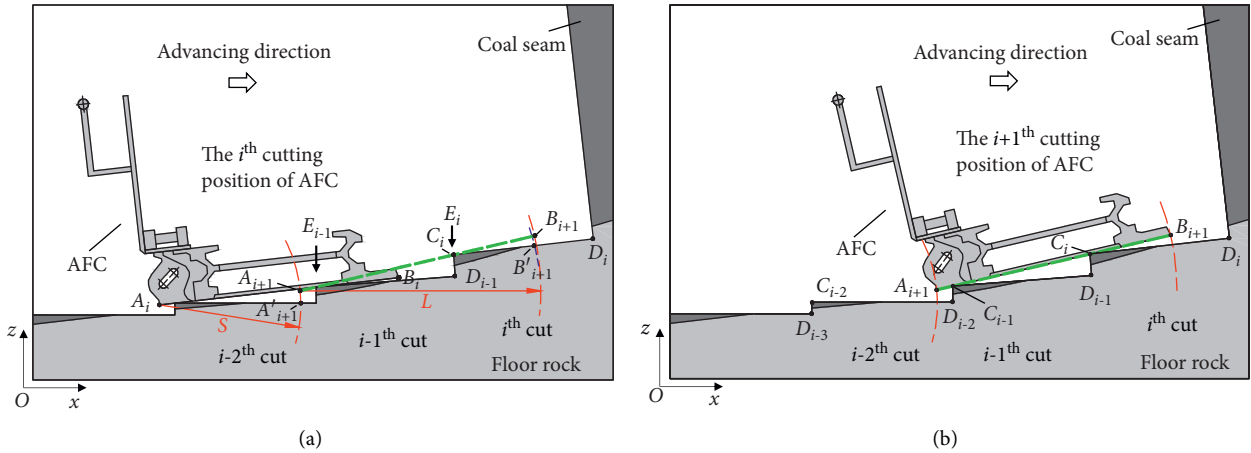


FIGURE 5: Schematic diagram of simulated AFC advancing. (a) Position of AFC before advancing. (b) Position of AFC after advancing.

When both $F(E_{i-1})$ and $F(E_i)$ are negative, the floor steps do not affect the position of AFC. After advancing, points A_{i+1} and B_{i+1} are equal to points A_{i+1}' and B_{i+1}' , respectively. Else, the difference between $F(E_{i-1})$ and $F(E_i)$, denoted by Δ , can be calculated as

$$\Delta = F(E_{i-1}) - F(E_i). \quad (6)$$

If $\Delta \leq 0$, the slope ($k_{A_{i+1}'E_i}$) of line $A_{i+1}'E_i$ is compared with the slope ($k_{E_{i-1}E_i}$) of line $E_{i-1}E_i$. If $k_{A_{i+1}'E_i} \leq k_{E_{i-1}E_i}$, after

advancing, point A_{i+1} is equal to A_{i+1}' , and the coordinates of point B_{i+1} are calculated by the following equation:

$$\begin{cases} (x_{B_{i+1}} - x_{A_{i+1}'})^2 + (z_{B_{i+1}} - z_{A_{i+1}'})^2 = L^2, \\ \frac{z_{B_{i+1}} - z_{E_i}}{x_{B_{i+1}} - x_{E_i}} = k_{A_{i+1}'E_i}, \\ x_{B_{i+1}} > x_{E_i}. \end{cases} \quad (7)$$

If $k_{A_{i+1}E_i} > k_{E_{i-1}E_i}$, after advancing, the coordinates of points A_{i+1} and B_{i+1} are calculated by the following equation:

$$\left\{ \begin{array}{l} (x_{A_{i+1}} - x_{A_i})^2 + (z_{A_{i+1}} - z_{A_i})^2 = S^2, \\ (x_{B_{i+1}} - x_{A_{i+1}})^2 + (z_{B_{i+1}} - z_{A_{i+1}})^2 = L^2, \\ \frac{z_{A_{i+1}} - z_{E_{i-1}}}{x_{A_{i+1}} - x_{E_{i-1}}} = \frac{z_{B_{i+1}} - z_{E_i}}{x_{B_{i+1}} - x_{E_i}} \\ = k_{E_{i-1}E_i}, \\ x_{A_{i+1}} > x_{A_i}, \\ x_{B_{i+1}} > x_{E_i}. \end{array} \right. \quad (8)$$

The slope ($k_{E_{i-1}E_i}$) of line $E_{i-1}E_i$ is compared with the pitch slope (k_i) of AFC for $\Delta > 0$. If $k_{E_{i-1}E_i} \geq k_i$, after advancing, the coordinates of points A_{i+1} and B_{i+1} are also calculated by equation (8). If $k_{E_{i-1}E_i} < k_i$, after advancing, since the pitch slope of AFC is not less than that of the $i-1$ th floor step ($k_{i+1} \geq k_{i-1}$), the coordinates of points A_{i+1} and B_{i+1} are calculated by equation (9) or (10).

$$\left\{ \begin{array}{l} (x_{A_{i+1}} - x_{A_i})^2 + (z_{A_{i+1}} - z_{A_i})^2 = S^2, \\ (x_{B_{i+1}} - x_{A_{i+1}})^2 + (z_{B_{i+1}} - z_{A_{i+1}})^2 = L^2, \\ \frac{z_{B_{i+1}} - z_{C_i}}{x_{B_{i+1}} - x_{C_i}} = k_i, \\ \frac{z_{E_{i-1}} - z_{A_{i+1}}}{x_{E_{i-1}} - x_{A_{i+1}}} = \frac{z_{B_{i+1}} - z_{E_{i-1}}}{x_{B_{i+1}} - x_{E_{i-1}}} > k_{i-1}, \\ x_{A_{i+1}} > x_{A_i}, \\ x_{B_{i+1}} > x_{C_i}, \end{array} \right. \quad (9)$$

$$\left\{ \begin{array}{l} (x_{A_{i+1}} - x_{A_i})^2 + (z_{A_{i+1}} - z_{A_i})^2 = S^2, \\ (x_{B_{i+1}} - x_{A_{i+1}})^2 + (z_{B_{i+1}} - z_{A_{i+1}})^2 = L^2, \\ \frac{z_{E_{i-1}} - z_{A_{i+1}}}{x_{E_{i-1}} - x_{A_{i+1}}} = \frac{z_{B_{i+1}} - z_{E_{i-1}}}{x_{B_{i+1}} - x_{E_{i-1}}} = k_{i-1}, \\ x_{A_{i+1}} > x_{A_i}, \\ x_{B_{i+1}} > x_{C_i}. \end{array} \right. \quad (10)$$

5. Cutting Path Planning Optimization Algorithm

According to the above introduction, the floor step of each cutting can be adjusted within the adjustment range of the trailing drum. Therefore, a multitree structure [29–32] is employed to store the possible advancing path of each cutting. At the same time, the depth-first search algorithm [33, 34] is utilized to analyze the advancing path of subsequent successive n cuttings for obtaining the optimal advancing path meeting the technological mining requirements.

Multitree is a data structure that stores hierarchical information. Each node can have zero or more child nodes, while it has only one parent node except the root node. A node with a maximum of two child nodes is called a binary tree, while a node with more than two child nodes is called a multitree. Figure 6 shows a multitree structure. Node A has no parent node and is the root node, while the nodes B, C, D, E, and F are the child nodes. B and C are the child nodes of A, while D, E, and F are the child nodes of C. Since node B has no child nodes, it is a leaf node.

Each node should be visited using the multitree structure, which is called the traversal process. The order of traversing nodes differs for different requirements and can be divided into breadth-first search and depth-first search. Breadth-first search means to search from the root node layer by layer. When all the nodes in the upper layer have been searched, it goes to the next layer to search until all nodes are traversed to find the desired results, such as $A \rightarrow B, C \rightarrow D, E, F$. Depth-first search refers to starting from the root node, following a branch path to the end and then returning to the child node of the upper layer and following another branching path to the end again until all nodes visit once, for example, $A \rightarrow B \rightarrow D \rightarrow E \rightarrow F \rightarrow C$.

From the initial position of the shearer, multiple possible advancing paths (floor steps with different heights) can be obtained corresponding to the first cutting within the allowable adjustment range by adjusting the trailing drum. Each possible advancing path can correspond to multiple possible advancing paths of the second cutting. As shown in Figure 7, the paths are calculated layer by layer to form a tree structure.

Taking the initial position of the shearer as the root node o , the multiple possible advancing paths (floor steps with different heights) of the first cutting are child nodes a_1, a_2, \dots, a_m , while each child node's path corresponds to multiple advancing paths of the subsequent cutting as child nodes. Thus, these path data meet the multitree data structure characteristics, and each advancing path is utilized as the node data to form a multitree, as shown in Figure 8.

In this paper, each possible advancing path of the successive n cuttings should be compared with the coal seam bottom boundary (extracted from the local high-precision 3D dynamic geological model ahead of the working face) to calculate the sandwiched area. Therefore, the depth-first search algorithm is selected to traverse the node data. As shown in Figure 9, a comparison between the retaining

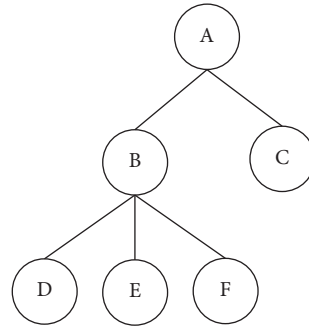


FIGURE 6: Schematic diagram of the multintree structure.

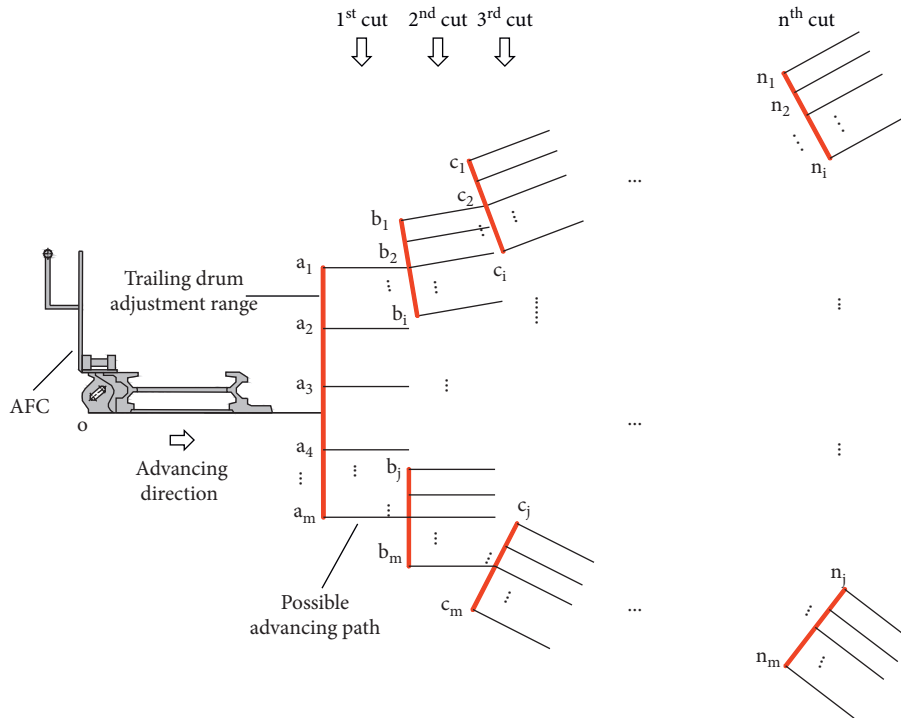


FIGURE 7: Schematic diagram of all possible advancing paths.

bottom coal area and the floor dinting area corresponding to each possible advancing path indicates that the advancing path that meets the process requirements is the optimal advancing path.

The actual mining conditions can be employed to plan the optimal advancing path according to the following three principles. (1) If the mining process requires cutting along the bottom boundary of the coal seam while cutting more coal and less rock, the branch path with the minimum sum of the retaining bottom coal area and the floor dinting area is the optimal path. (2) If the maximum recovery of coal resources is required, the branch path with zero retaining bottom coal area and minimum floor dinting area is the optimal path. (3) If minimum cutting rock layers are required, the branch path with zero floor dinting area and minimum retaining bottom coal area is the optimal path.

In the optimal advancing path of each connection position of the middle groove, the starting points of the floor

steps are connected in an orderly manner, as the corresponding cutting path of the trailing drum. As shown in Figure 10, all possible advancing paths of each connection position can be calculated sequentially from one end of the working face to the other one. First, the optimal advancing paths of point 1 and point 2 are calculated based on the advancing direction constraints. Second, in order to calculate the optimal advancing path at point 3, each floor step should be considered comprehensively with the corresponding steps of the advancing path of points 1 and 2 to meet the AFC vertical curvature. Similarly, the calculation of the optimal advancing path for each subsequent point should be comprehensively considered with the optimal advancing path of the previous two points to meet the AFC vertical curvature until the other end of the working face. Finally, all the starting points of the first cut floor step are connected, which forms the planning cutting path of the trailing drum for the next cutting. The planning cutting

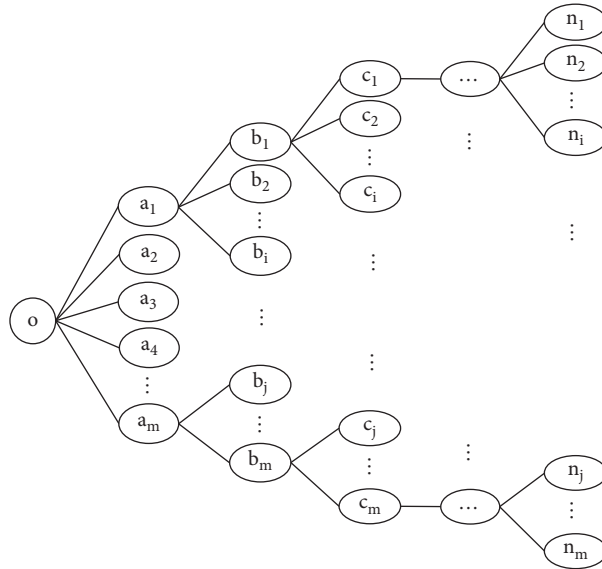


FIGURE 8: Schematic diagram of the multitree data structure of the advancing path.

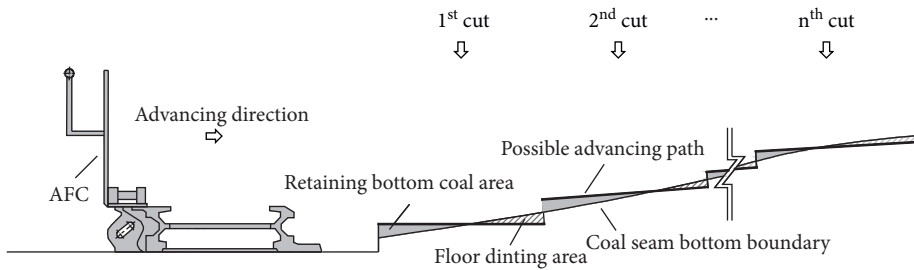


FIGURE 9: Schematic diagram of retaining bottom coal area and the floor dinting area.

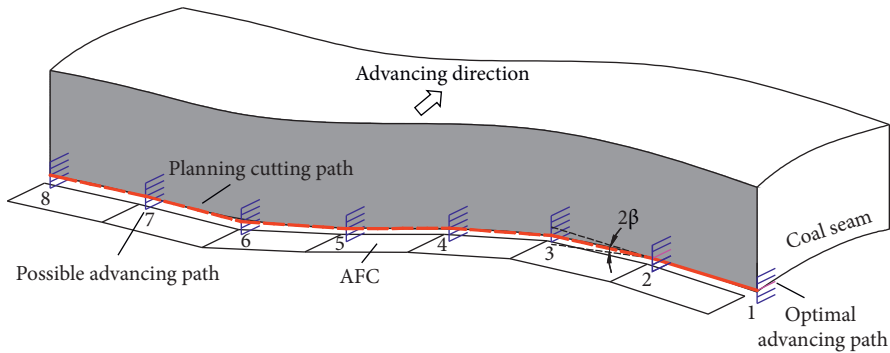


FIGURE 10: Schematic diagram of the planning cutting path of the trailing drum.

paths of the trailing drum for the subsequent successive n cuttings can be obtained similarly.

6. Results and Discussion

Taking a working face of Guotun Coal Mine as an example, the optimal advancing path is compared with the “memory cut” advancing path. The working face of Guotun Coal Mine is a longwall working face, in which the face width is 188 m, the coal seam thickness is 4.2–6.0 m, and the coal seam dip

angle is 0–15°, equipped with MG900/2245-GWD coal shearer and SGZ1000/2000 AFC. The shearer has a cutting depth of 0.8 m and a maximum floor-based quantity of 39 cm. A dip angle less than or equal to 15° is suitable for coal seams. The bottom width of AFC is 1.665 m, while the distance between the ramp plate and the coal wall is 44 cm. It is assumed that the drum adjustment interval is 2 cm, while the maximum adjustment height is 10 cm, and the maximum height of the floor step is 5 cm. LongRuanGIS 3.2 of Longruan is utilized to construct the high-precision 3D

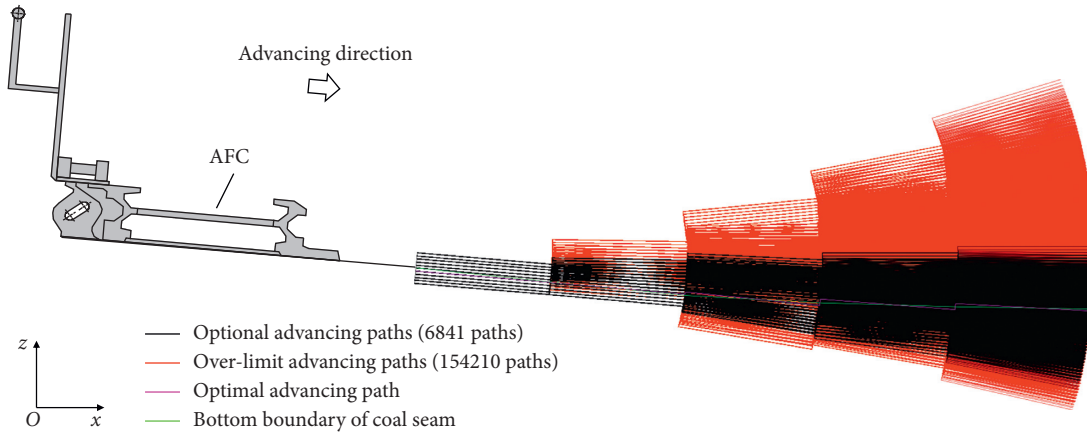
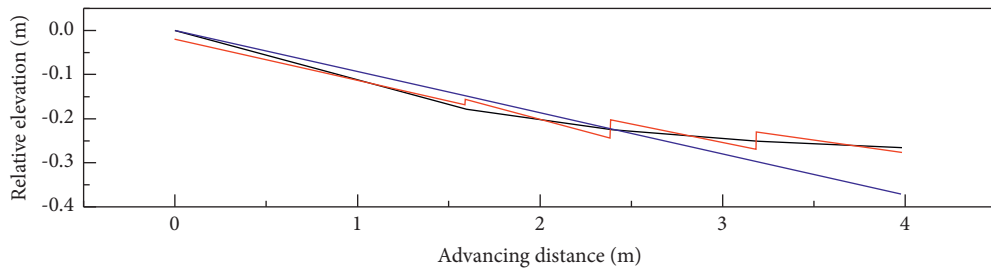
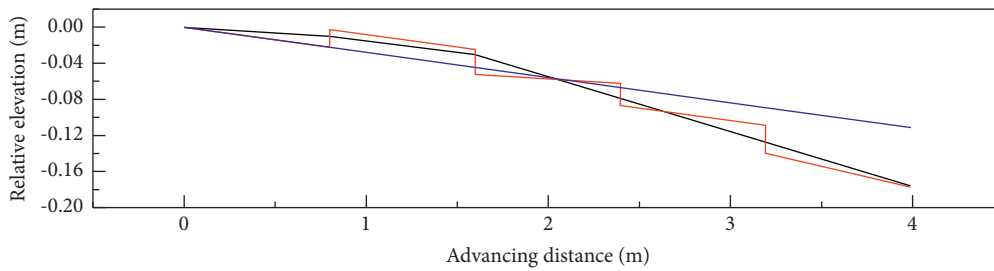


FIGURE 11: Schematic diagram of the optimal advancing path of the shearer for subsequent five cuttings.



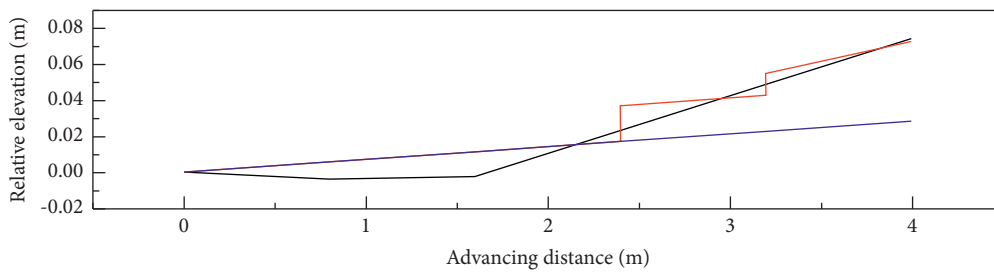
— Bottom boundary of coal seam
 — Optimal advancing path
 — “Memory cut” advancing path

(a)



— Bottom boundary of coal seam
 — Optimal advancing path
 — “Memory cut” advancing path

(b)



— Bottom boundary of coal seam
 — Optimal advancing path
 — “Memory cut” advancing path

(c)

FIGURE 12: Continued.

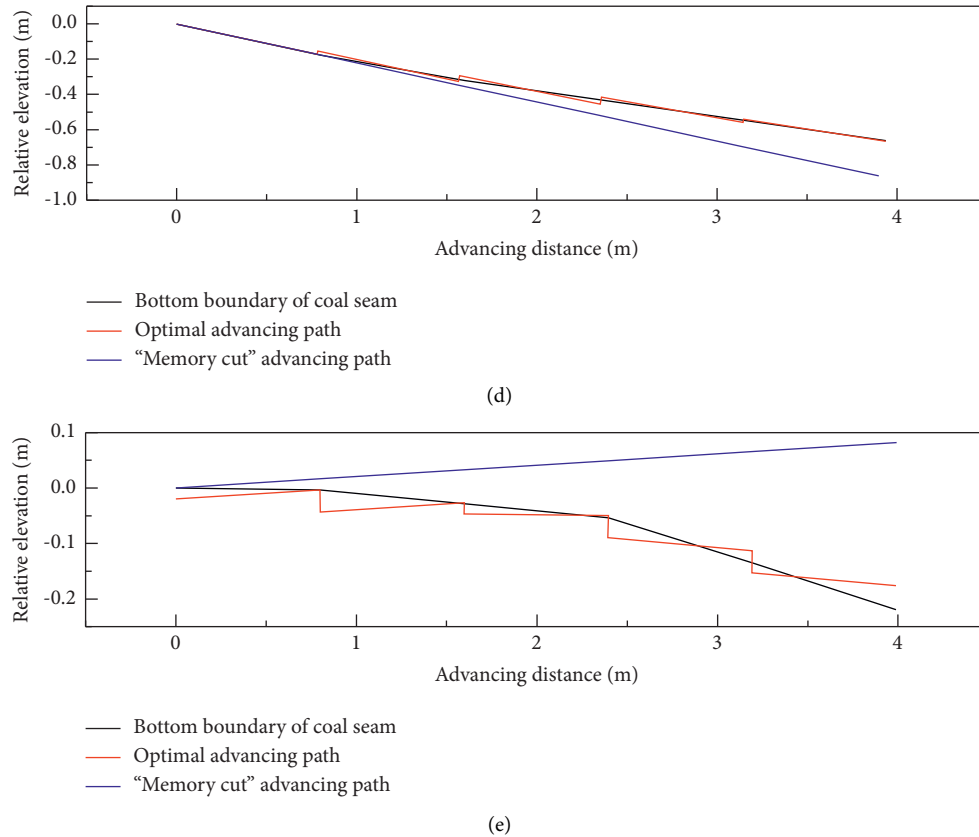


FIGURE 12: Comparison of two cutting paths at different positions: (a) sample point a; (b) sample point b; (c) sample point c; (d) sample point d; (e) sample point e.

geological model according to all the actual geological data of the coal seam of the panel. A section of the coal seam bottom boundary is chosen arbitrarily from the local model ahead of the working face for testing. The initial pitch angle of the shearer is -5.35° , and all possible advancing paths for the successive five cuttings are shown in Figure 11. The overlimit paths are screened out using constraint conditions, such as the maximum pitch angle of the shearer and the maximum height of the floor step. Among the remaining optional paths, the optimal advancing path is calculated based on the principle of “cutting along the coal seam bottom boundary and cutting more coal and less rock.”

The optimal advancing path in Figure 11 is extracted (see Figure 12(a)), while the other nine optimal paths are calculated in the working face using the same principle, and some of these paths are shown in Figure 12. Simultaneously, the “memory cut” advancing paths are simulated for comparison. The comparison results are presented in Table 1. The “memory cut” advancing paths are performed by manually controlling one cut along the bottom boundary of the coal seam and automatically cutting four cuts.

According to Figure 12, the optimal advancing path can better fit the coal seam bottom boundary than the “memory cut” advancing path under the principle of “cutting along the coal seam bottom boundary and cutting more coal and less rock.” Compared with floor dinting and retaining bottom coal, the proposed optimal advancing path has apparent

advantages over “memory cut.” The total amount of floor dinting and retaining bottom coal is reduced by 79.58% on average. Adopting the optimal advancing path leads to the rapid mining of the intelligent working face and reduces resource waste. It is necessary to reduce the number of automatic cutting and increase the number of manual control cuttings to achieve similar results with “memory cut” technology.

The dip angle of the coal seam bottom boundary is recorded at the starting position of each cutting and the end position of the last cutting in the sample, as shown in Table 2. According to the optimization effect of the optimal advancing path in Table 1, the following results can be drawn:

- (1) The optimal propulsion path can be utilized for coal seams with various dip angles.
- (2) Compared with the “memory cut” technology, the advantage of the optimal advancing path is more evident for the coal seam with the more significant dip angle variations.
- (3) As shown in Figure 13, there is a roughly positive correlation between the optimization effect of the optimal advancing path and the change of coal seam dip angle.

This paper only studies the cutting path planning optimization algorithm of the trailing drum for subsequent

TABLE 1: Comparison of the two advancing methods (unit: m^2).

Sample point	Optimal cut			Memory cut			Optimization rate
	Floor dinting area	Retaining bottom coal area	Total	Floor dinting area	Retaining bottom coal area	Total	
a	0.0197	0.0170	0.0369	0.0784	0.0356	0.1140	67.61%
b	0.0165	0.0134	0.0299	0.0186	0.0638	0.0825	63.78%
c	0.0016	0.0228	0.0244	0.0425	0.0170	0.0596	58.95%
d	0.0090	0.0147	0.0238	0.2911	0	0.2911	91.84%
E	0.0406	0.0158	0.0564	0	0.4308	0.4308	86.92%
F	0.0141	0.0127	0.0269	0.0321	0	0.0321	16.26%
g	0.0094	0.0067	0.0161	0	0.0854	0.0854	81.12%
h	0.0096	0.0155	0.0251	0	0.1663	0.1663	84.88%
i	0.0183	0.0200	0.0383	0.0184	0.1361	0.1545	75.24%
j	0.0068	0.0130	0.0198	0.0405	0	0.0405	51.15%
Average	0.0146	0.0152	0.0298	0.0522	0.0935	0.1457	79.58%

TABLE 2: Statistical data of dip angle of coal seam bottom boundary (unit: $^\circ$).

Sample point	Starting point of each cutting					End point of the 5 th cut	Average	Standard deviation
	1 st cut	2 nd cut	3 rd cut	4 th cut	5 th cut			
a	-6.39	-6.39	-4.18	-1.89	-1.23	-1.06	-3.52	2.27
b	-0.73	-0.95	-3.50	-3.50	-3.50	-3.50	-2.61	1.26
c	-0.28	-0.28	1.83	1.83	1.83	1.83	1.13	0.99
d	-12.53	-10.96	-8.38	-8.32	-8.32	-8.32	-9.47	1.67
e	-0.25	-1.81	-1.81	-5.86	-6.06	-6.06	-3.64	2.41
f	-7.89	-8.15	-8.15	-8.15	-8.15	-8.15	-8.11	0.10
g	-2.30	-2.62	-3.13	-3.31	-3.31	-3.31	-3.00	0.40
h	-3.22	-3.87	-5.52	-5.52	-5.52	-5.52	-4.86	0.95
i	-4.20	-5.96	-8.57	-8.57	-8.58	-8.58	-7.41	1.72
j	-7.45	-7.41	-7.41	-7.41	-7.06	-7.06	-7.30	0.17

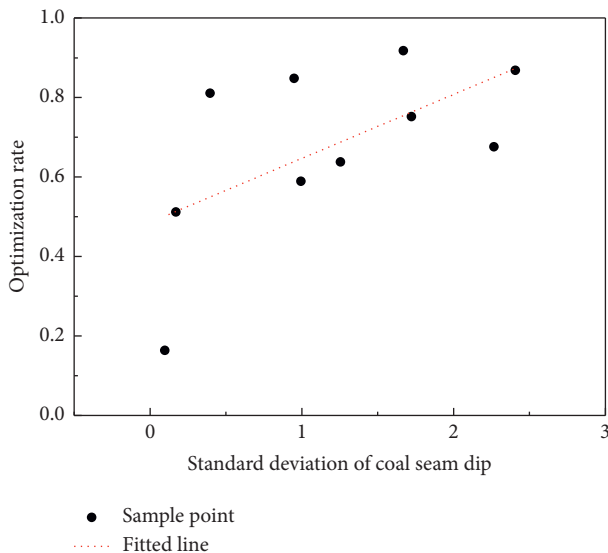


FIGURE 13: The relationship between the optimization rate and the standard deviation of coal seam dip angle.

successive n cuttings using the local high-precision 3D dynamic geological model ahead of the working face and lacks the corresponding cutting path of the leading drum.

Accordingly, the cutting path of the leading drum should be planned based on the cutting paths of the trailing drum, while considering various factors, such as coal seam thickness, mining height, working face roof condition, hydraulic support top beam inclination, and hydraulic supported area.

7. Conclusions

Higher requirements are put forward for the intelligent control of the shearer in the construction of intelligent coal mines. This paper employs the local high-precision 3D dynamic geological model to derive the shearer's cutting path planning optimization algorithm. The research results are mainly reflected in the following four points:

- (1) The "memory cut" technology does not plan the trailing drum cutting path, and the single cutting path optimization or prediction method based on the "memory cut" technology cannot meet the intelligent mining requirements. In order to solve the mentioned problems, this paper proposes a multicutting path planning algorithm, which can adapt to the mining face with different mining requirements and realize automatic operation. Furthermore, the algorithm can automatically re-plan the cutting path of the shearer for subsequent successive n cuttings with the dynamic

update of the local geological model or the continuous advancement of the working face.

- (2) The shearer's advancing path calculation requires careful consideration of constraints, such as the shearer pitch angle, the vertical curvature of AFC, and the height of the floor step, as well as the initial position and initial pitch angle of the shearer. Besides, the calculation method for the shearer's position after advancing can change with different floor steps. In this regard, this paper proposes a complete calculation method for the advancing path to simulate the shearer's advancing process.
- (3) Regarding how to achieve the optimal cutting of the trailing drum, this paper simulates all possible advancing paths under different adjustment values of the trailing drum and employs the multi-tree and the depth-first algorithm to compare all possible advancing paths of the subsequent successive n cuttings to obtain the optimal advancing path and realize the shearer pitch angle control. Meanwhile, this paper proposes to increase the constraint of the vertical curvature of AFC in the calculation process of the optimal advancing path. This means that the planned cutting curve for each cutting of the shearer trailing drum can be calculated while calculating the optimal advancing path at each connection position of the AFC.
- (4) Taking a working face of Guotun Coal Mine as an example, the principle of "cutting along the coal seam bottom boundary and cutting more coal and less rock" is employed to compare the optimal advancing path with the "memory cut" advancing path. The optimal advancing algorithm has evident advantages over the "memory cut" technology, especially for the more significant variations in the coal seam dip angle. The total amount of floor dinting and retaining bottom coal is reduced by 79.58% on average. The optimal advancing algorithm ensures the rapid advancement of the intelligent working face while reducing resource waste.

Data Availability

The geological data in this paper mainly come from the Guotun Coal Mine in Shandong Province of China. The geological model is constructed using LongRuanGIS 3.2 of Longruan. Because coal mine geographic data contain some confidential data, data cannot be shared. Requests for access to the data can be made to the corresponding author if it is necessary.

Conflicts of Interest

The authors declare that there are no conflicts of interest regarding the publication of this paper.

Acknowledgments

This study was supported by the State Key R&D Plan (2017YFC0804303) of the Ministry of Science and Technology of China.

References

- [1] K. Wang and F. Du, "Coal-gas compound dynamic disasters in China: a review," *Process Safety and Environmental Protection*, vol. 133, pp. 1–17, 2020.
- [2] F. Du and K. Wang, "Unstable failure of gas-bearing coal-rock combination bodies: insights from physical experiments and numerical simulations," *Process Safety and Environmental Protection*, vol. 129, pp. 264–279, 2019.
- [3] Y. Yuan, S. Z. Wang, W. M. Wang, and C. Zhu, "Numerical simulation of coal wall cutting and lump coal formation in a fully mechanized mining face," *International Journal of Coal Science and Technology*, vol. 8, pp. 1–13, 2021.
- [4] H. Shi, J. Xie, X. Wang, J. Li, and X. Ge, "An operation optimization method of a fully mechanized coal mining face based on semi-physical virtual simulation," *International Journal of Coal Science & Technology*, vol. 7, no. 1, pp. 147–163, 2020.
- [5] G. F. Wang, H. Wang, H. W. Ren et al., "2025 scenarios and development path of intelligent coal mine," *Journal of China Coal Society*, vol. 43, no. 2, pp. 295–305, 2018.
- [6] G. F. Wang and D. S. Zhang, "Innovation practice and development prospect of intelligent fully mechanized technology for coal mining," *Journal of China University of Mining & Technology*, vol. 47, no. 3, pp. 459–467, 2018.
- [7] G. F. Wang, G. R. Zhao, and H. W. Ren, "Analysis on key technologies of intelligent coal mine and intelligent mining," *Journal of China Coal Society*, vol. 44, no. 1, pp. 34–41, 2019.
- [8] M. Li, S. W. Yang, Z. M. Sun, and H. Wu, "Study on framework and development prospects of intelligent mine," *Coal Science and Technology*, vol. 45, no. 1, pp. 121–128+134, 2017.
- [9] S. J. Mao, J. J. Cui, J. S. Linghu, M. Li, Z. Sun, and H. Chen., "System design and key technology of transparent mine management and control platform," *Journal of China Coal Society*, vol. 43, no. 12, pp. 3539–3548, 2018.
- [10] S. J. Mao and M. Li, "Theory and application of gray geographic information system," *Datong Coal Science & Technology*, vol. 157, pp. 1–3+53, 2017.
- [11] S. J. Mao, "Gray geographical information system—the theory and technology of correct geological spatial data dynamically," *Acta Scientiarum Naturalium Universitatis Pekinensis*, vol. 38, no. 4, pp. 556–562, 2002.
- [12] J. Y. Cheng, M. B. Zhu, Y. H. Wang, H. Yue, and W. X. Cui, "Cascade construction of geological model of longwall panel for intelligent precision coal mining and its key technology," *Journal of China Coal Society*, vol. 44, no. 8, pp. 2285–2295, 2019.
- [13] W. L. Liu, X. L. Zhang, and S. B. Wang, "Modeling and dynamic correction technology of 3D coal seam model for coal-mining face," *Journal of China Coal Society*, vol. 45, no. 6, pp. 1973–1983, 2020.
- [14] S. S. Peng, F. Du, J. Cheng, and Y. Li, "Automation in U.S. longwall coal mining: a state-of-the-art review," *International Journal of Mining Science and Technology*, vol. 29, no. 2, pp. 151–159, 2019.
- [15] J. C. Wang, S. S. Peng, and Y. Li, "State-of-the-art in underground coal mining and automation technology in the United States," *Journal of China Coal Society*, vol. 46, no. 1, pp. 36–45, 2021.
- [16] J. C. Ralston, C. O. Hargrave, and M. T. Dunn, "Longwall automation: trends, challenges and opportunities," *International Journal of Mining Science and Technology*, vol. 27, no. 5, pp. 733–739, 2017.

- [17] J. C. Ralston, D. C. Reid, M. T. Dunn, and D. W. Hainsworth, "Longwall automation: d," *International Journal of Mining Science and Technology*, vol. 25, no. 6, pp. 865–876, 2015.
- [18] J. Ley, M. Beilstein, and C. LeViere, "Adaptive pitch steering in a longwall shearing system," 2018.
- [19] C. Tan, Z. P. Xu, and K. Niu, "Research on path planning of shearer memory cutting," *Morden Mining*, vol. 25, no. 12, pp. 41-42+53, 2009.
- [20] L. L. Zhang, C. Tan, Z. B. Wang, J. P. Mi, and W. C. Zhu, "Optimization of mnemonic cutting path for coal shearer Based on corpuscular group algorithm," *Coal Science and Technology*, vol. 38, no. 4, pp. 69–71, 2010.
- [21] G. T. Quan, C. Tan, H. C. Hou, and Z. Y. Wang, "Cutting path planning of coal shearer base on particle swarm triple spline optimization," *Coal Science and Technology*, vol. 39, no. 3, pp. 77–79, 2011.
- [22] L. L. Zhang, C. Tan, Z. B. Wang, X. F. Yang, and J. P. Mi, "Optimization of shearer memory cutting path based on genetic algorithm," *Coal Engineering*, vol. 2, pp. 111–113, 2011.
- [23] Y. W. Liang, *Theory and Technology of Intelligent Control for Shearer Steering*, Taiyuan University of Technology, Taiyuan, China, 2005.
- [24] Z. B. Wang and Z. P. Xu, "Research on the technology of shearer self-adaptive memory cutting," in *Proceedings of the 2009 Second International Conference on Intelligent Computation Technology and Automation*, pp. 920–923, Changsha, Hunan, October 2009.
- [25] Z. P. Xu, *Study on the Key Technologies of Self-Adaptive Cutting for Shearer*, China University of Mining and Technology, 2011.
- [26] B. Zhou and Z. B. Wang, "Application of grey system theory to memory cutting technology of coal shearer," *Coal Science and Technology*, vol. 39, no. 3, pp. 74–76+99, 2011.
- [27] L. Si, Z. B. Wang, X. H. Liu, and C. Tan, "Cutting path planning of coal mining machine based on prediction of coal seam distribution," *Journal of China University of Mining & Technology*, vol. 43, no. 3, pp. 464–471, 2014.
- [28] S. R. Ge, X. D. Hao, K. Tian, C. Gao, and L. K. Le, "Principle and key technology of autonomous navigation cutting for deep coal seam," *Journal of China Coal Society*, vol. 46, no. 3, pp. 774–788, 2021.
- [29] D. Kim, B. Y. Song, and J. B. Kim, "Multi-tree-based path planning of robotic manipulators for unstructured depalletizing tasks," *Journal of Institute of Control, Robotics and Systems*, vol. 26, no. 4, pp. 263–268, 2020.
- [30] B. M. Suhng and W. Lee, "A new link-based single tree building algorithm for shortest path searching in an urban road transportation network," *Journal of Electrical Engineering and Technology*, vol. 8, no. 4, pp. 889–898, 2013.
- [31] Y. Zhao, X. C. Zhang, and T. J. Kang, "An ant colony algorithm based on multi-way tree for optimal site location," *Acta Geographica Sinica*, vol. 66, no. 2, pp. 279–286, 2011.
- [32] D. C. Shu and G. W. Cheng, "Traversal algorithm based on multi-subtrees and its application on the topological relationship in digital drainage network," *Resources and Environment in the Yangtze Basin*, vol. 15, no. 6, pp. 733–739, 2006.
- [33] S. J. Shi, "Discussion on search algorithm," *Computer Knowledge an Technology*, vol. 16, no. 23, pp. 216–217, 2020.
- [34] G. P. W. Rodrigues, L. H. M. Costa, G. M. Farias, and M. A. H. De Castro, "A depth-first search algorithm for optimizing the gravity pipe networks layout," *Water Resources Management*, vol. 33, no. 13, pp. 4583–4598, 2019.